

# Organo-noble-gas hydride compounds HKrCCH, HXeCCH, HXeCC, and HXeCCXeH: Formation mechanisms and effect of $^{13}\text{C}$ isotope substitution on the vibrational properties

Hanna Tanskanen,<sup>a)</sup> Leonid Khriachtchev, Jan Lundell, and Markku Räsänen  
*Department of Chemistry, University of Helsinki, P.O. Box 55, FIN-00014 Helsinki, Finland*

(Received 8 June 2004; accepted 6 August 2004)

We investigate the formation mechanism of HXeCCXeH in a Xe matrix. Our experimental results show that the HXeCCXeH molecules are formed in the secondary reactions involving HXeCC radicals. The experimental data on the formation of HXeCCXeH is fully explained based on the model involving the  $\text{HXeCC} + \text{Xe} + \text{H} \rightarrow \text{HXeCCXeH}$  reaction. This reaction is the first case when a noble-gas hydride molecule is formed from another noble-gas molecule. In addition, we investigate the  $^{12}\text{C}/^{13}\text{C}$  isotope effect on the vibrational properties of organo-noble-gas hydrides (HKrCCH, HXeCCH, HXeCC, and HXeCCXeH) in noble-gas matrixes. The present experimental results and *ab initio* calculations on carbon isotope shifts of the vibrational modes support the previous assignments of these molecules. Upon  $^{12}\text{C}$  to  $^{13}\text{C}$  isotope substitution, we observed a pronounced effect on the H-Kr stretching mode of HKrCCH (downshift of  $1.0\text{--}3.6\text{ cm}^{-1}$ , depending on the matrix site) and a small anomalous shift ( $+0.1\text{ cm}^{-1}$ ) of the H-Xe stretching mode of HXeCCH and HXeCCXeH. © 2004 American Institute of Physics. [DOI: 10.1063/1.1799611]

## I. INTRODUCTION

About 10 years ago the Helsinki group introduced the first HNgY molecules (Ng=a noble-gas atom and Y=electronegative fragment).<sup>1</sup> These chemically bound HNgY molecules can be prepared in low-temperature noble-gas matrixes using UV photolysis of the HY precursor and subsequent thermal mobilization of the H atoms.<sup>2,3</sup> The use of this procedure has led to preparation of 20 new chemical hydride compounds. The recent findings include compounds such as HArF,<sup>4</sup> HXeO,<sup>5</sup> and a group of organo-noble-gas hydrides (HXeCCH, HXeCC, HXeCCXeH, HKrCCH, HKrC<sub>4</sub>H, HXeC<sub>4</sub>H).<sup>6–9</sup>

The HNgY molecules are formed from the neutral H + Ng + Y fragments and thermal mobility of atomic hydrogen controls the formation of HNgY molecules in solid noble gases.<sup>2,3</sup> Thermal diffusion of atomic hydrogen in noble-gas solids has been repeatedly studied. Eberlein and Creutzburg extracted the activation energies of 123 and 66 meV for mobility of atomic hydrogen in Xe and Kr matrixes.<sup>10</sup> Vaskonen *et al.* measured the activation energy of 90–140 meV for this process in solid Kr.<sup>11</sup> Since the formation of HNgY molecules is diffusion controlled, the thermal mobility of atomic hydrogen can be investigated in noble-gas solids using the HNgY molecules as a probe, and this method has been successfully used for the cases of HXeH and HXeOH in solid Xe and HKrCl in solid Kr.<sup>12,13</sup> In those studies, the mobilities of H and D atoms in Xe and Kr matrixes were clearly distinguished and the difference between the activation energies was estimated to be  $\sim 4\text{ meV}$ .<sup>12,13</sup>

The annealing-induced formation of HNgY molecules consumes a large part of H atoms produced during photolysis

of the HY precursor.<sup>2,3</sup> The experimental data on HKrCl in solid Kr and on HXeH in solid Xe reveal further reactions (secondary reactions) of the HNgY molecules with mobile H atoms.<sup>13,14</sup> A simple kinetic model including the formation reactions of HNgY molecules and the reactions of the HNgY molecules and mobile H atoms described the experimental observations. It was suggested that these secondary reactions limit the amounts of HNgY molecules formed upon annealing and presumably resulted in formation of H<sub>2</sub> molecules.

The HNgY molecules can be easily detected by IR absorption spectroscopy due to their extremely intense H-Ng stretching absorption, and the characterization is supported by *ab initio* theoretical methods.<sup>2,3</sup> Isotope substitution is frequently used to verify the experimental assignment. The usual harmonic isotope effect is a downshift of the vibrational frequencies when the reduced mass increases. In the case of HNgY molecules the H/D isotope substitution has produced normal downshifts of the H-Ng stretching absorption in a good agreement with the harmonic calculations. Recently, we have observed an anomalous isotope effect for HXeOH and HXeOD molecules and for HXeO radical upon  $^{16}\text{O}/^{18}\text{O}$  isotope substitution.<sup>5,15</sup> Experiments with  $^{18}\text{O}$ -substituted water showed small but noticeable blueshifts of the H-Xe stretching vibration frequency of these molecules. We described this effect theoretically in terms of anharmonic coupling between the normal modes.<sup>15</sup> This image was confirmed by Yu and Muckerman in their high-level *ab initio* calculations on HXeOH.<sup>16</sup>

In the present work, we investigate the  $^{12}\text{C}/^{13}\text{C}$  isotope effect on the vibrational properties of HKrCCH, HXeCCH, HXeCC, and HXeCCXeH. These isotope-substitution studies support the previous assignments of these molecules<sup>6,7</sup> and reveal a relatively large effect on the H-Kr stretching mode of the HKrCCH molecule and a small anomalous effect on

<sup>a)</sup>Electronic mail: [hanna.tanskanen@helsinki.fi](mailto:hanna.tanskanen@helsinki.fi)

TABLE I. Calculated MP2/LJ18(Xe),6-311++G(2*d*,2*p*) vibrational frequencies (in cm<sup>-1</sup>) and IR intensities [in parentheses (in km mol<sup>-1</sup>)] of <sup>12</sup>C/<sup>13</sup>C-substituted HNgCCH (Ng=Kr or Xe) and HXeCCXeH. For HXeCC, the computational level is CCSD(T)/LJ18(Xe),6-311++G(2*d*,2*p*).

	MP2/6-311++G(2 <i>d</i> ,2 <i>p</i> )			MP2/LJ18(Xe),6-311++G(2 <i>d</i> ,2 <i>p</i> )			
	HKr <sup>12</sup> C <sup>12</sup> CH	HKr <sup>13</sup> C <sup>13</sup> CH	Shift ( <sup>13</sup> C)	HXe <sup>12</sup> C <sup>12</sup> CH <sup>b</sup>	HXe <sup>13</sup> C <sup>13</sup> CH	Shift ( <sup>13</sup> C)	
C-H str.	3454.9(33.9)	3438.1(32.2)	-16.8	C-H str.	3462.3(30.7)	3445.5(29.5)	-16.8
C-C str.	1959.6(3.9)	1888.6(4.4)	-71.0	C-C str.	1970.5(5.8)	1899.0(5.4)	-71.5
H-Kr str.	1464.3(2368.7)	1464.1(2372.2)	-0.2	H-Xe str.	1735.9(1515.3)	1735.8(1517.1)	-0.1
Bend <sup>a</sup>	697.5(2.4)	696.1(2.4)	-1.4	Bend <sup>a</sup>	687.8(38.5)	686.4(37.6)	-1.4
Bend <sup>a</sup>	651.8(44.4)	645.9(44.7)	-5.9	Bend <sup>a</sup>	640.6(27.3)	634.9(27.9)	-5.7
Kr-C str.	322.7(194.3)	313.4(183.1)	-9.3	Xe-C str.	327.2(171.7)	316.9(160.9)	-10.3
Bend <sup>a</sup>	132.3(19.3)	128.1 (18)	-4.2	Bend <sup>a</sup>	131.4(14.6)	127.2(13.6)	-4.2
	CCSD(T)/LJ18(Xe),6-311++G(2 <i>d</i> ,2 <i>p</i> )			MP2/LJ18(Xe),6-311++G(2 <i>d</i> ,2 <i>p</i> )			
	HXe <sup>12</sup> C <sup>12</sup> C	HXe <sup>13</sup> C <sup>13</sup> C	Shift ( <sup>13</sup> C)	HXe <sup>12</sup> C <sup>12</sup> CXeH <sup>b</sup>	HXe <sup>13</sup> C <sup>13</sup> CXeH	Shift ( <sup>13</sup> C)	
C-C str.	1599.0	1536.3	-62.7	C-C str.	1967.9 (0)	1890.6 (0)	-77.3
H-Xe str.	1754.7	1754.3	-0.4	Xe-H sym. str.	1670.8 (0)	1670.8 (0)	0
H-Xe-C bend	641.0 <sup>a</sup>	640.9	-0.1	Xe-H asym. str.	1594.7(5450.5)	1594.5(5467.2)	-0.2
		639.9	-1.1	Bend <sup>a</sup>	667.1(47.5)	665.6(46.5)	-1.5
Xe-C-C bend	388.9 <sup>a</sup>	373.9	-15.0	Bend <sup>a</sup>	651.6 (0)	650.1 (0)	-1.5
		373.7	-15.2	Xe-C asym. str.	454.2(735.3)	437.8(682.0)	-16.4
Xe-C str.	273.2	264.1	-9.1	Bend <sup>a</sup>	129.7 (0)	129.7 (0)	0
				Xe-C sym. str. <sup>a</sup>	60.3(11.0)	58.2(10.3)	-2.1
				Bend <sup>a</sup>	48.1 (0)	46.3 (0)	-1.8

<sup>a</sup>Doubly degenerate.<sup>b</sup>From Ref. 19.

the H-Xe stretches of HXeCCH and HXeCCXeH. In addition, we study the formation mechanism of the HXeCCXeH molecule. Our experimental results show that the HXeCCXeH molecules are formed in secondary reactions involving HXeCC radicals.

## II. CALCULATIONS

### A. Computational details

The calculations were carried out with the GAUSSIAN98 (revision A.11.4) package of computational codes.<sup>17</sup> For HNgCCH (Ng=Kr or Xe) and HXeCCXeH, the Møller-Plesset second order perturbation theory (MP2) was used for electron correlation. For HXeCC, the CCSD(T) method was employed. The relativistic pseudopotentials (ECP) by LaJohn *et al.* were taken for Xe. These ECP include the *d* subshell in the valence space resulting in 18 valence electrons. The basis set was used in a decontracted form and it is denoted as LJ18.<sup>18</sup> The standard split valence 6-311++G(2*d*,2*p*) basis set was used for hydrogen, carbon, and krypton. The harmonic vibrational frequencies were calculated analytically for the MP2 method and numerically for the CCSD(T) method.

### B. Computational results

The calculated harmonic frequencies for <sup>12</sup>C- and <sup>13</sup>C-substituted HNgCCH (Ng=Kr or Xe), HXeCC, and HXeCCXeH are presented in Table I. The values for HXe<sup>12</sup>C<sup>12</sup>CH and HXe<sup>12</sup>C<sup>12</sup>CXeH are from Ref. 19. The harmonic calculations show downshifts in energy for all vibrational modes of the <sup>13</sup>C-substituted molecules as compared with the <sup>12</sup>C species. For HNgCCH compounds with Kr and Xe, the computational shifts of various frequencies are quite

similar: the C-H stretch shifts by -16.8 cm<sup>-1</sup> for both compounds, and the shift of the C-C-H bend is -5.9 cm<sup>-1</sup> for HKrCCH and -5.7 cm<sup>-1</sup> for HXeCCH. The downshift of the H-Ng stretch upon <sup>13</sup>C isotope substitution is very small, and it is -0.2 cm<sup>-1</sup> for HKrCCH and -0.1 cm<sup>-1</sup> for HXeCCH. The H-Xe stretching vibration of HXeCCXeH shifts by -0.2 cm<sup>-1</sup>, which is similar to HNgCCH, the bending mode of HXeCCXeH shifts by -1.5 cm<sup>-1</sup> and the Xe-C asymmetric stretching mode frequency decreases by 16.4 cm<sup>-1</sup>. For HXeCC, according to the CCSD(T) calculations, the H-Xe stretching, C-C stretching, and Xe-C-C bending modes shift by -0.4, -62.7, and -15.0 cm<sup>-1</sup>, respectively.

## III. EXPERIMENT

### A. Experimental details

The <sup>12</sup>C<sub>2</sub>H<sub>2</sub>/Ng and <sup>13</sup>C<sub>2</sub>H<sub>2</sub>/Ng (<sup>13</sup>C-substituted acetylene from Icon Services, <sup>13</sup>C purity of 99%, Ng=Kr or Xe) samples were deposited from the gas phase onto a CsI window cooled by a closed-cycle helium cryostat (DE-202A, APD) at 20 K for Kr and at 30 K for Xe. The matrix ratios were ~1:1000-1:2000 and in the <sup>13</sup>C<sub>2</sub>H<sub>2</sub>/Ng samples no sign of the mixed form (H<sup>12</sup>C<sup>13</sup>CH) was visible in the absorption spectra. The matrix thickness was typically ~100 μm. The IR absorption spectra (4000-400 cm<sup>-1</sup>) were measured with a Nicolet 60 SX Fourier transform infrared spectrometer with 1 cm<sup>-1</sup> resolution coadding 500 scans. Photodecomposition of acetylene was carried out using an excimer laser (MPB, MSX-250) operating at 193 nm (ArF) and an optical parametric oscillator (Continuum, OPO Sunlite FX-1) at 250 nm.

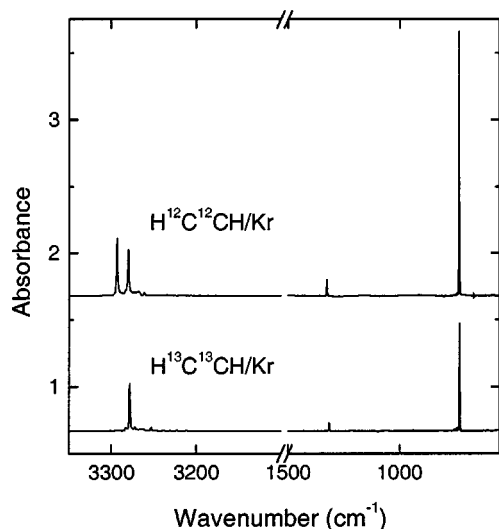


FIG. 1. IR absorption spectra of acetylene in solid Kr at 8 K. Spectra for  $^{12}\text{C}_2\text{H}_2$  and  $^{13}\text{C}_2\text{H}_2$  are shown by the upper and lower traces, respectively.

## B. Experimental results

The IR absorption spectra of  $^{12}\text{C}_2\text{H}_2$  (the strongest absorptions at 3293, 3280, 1325.5, and  $732\text{ cm}^{-1}$ ) and  $^{13}\text{C}_2\text{H}_2$  (the strongest absorptions at 3278.5, 1315, and  $730.5\text{ cm}^{-1}$ ) in solid Kr are presented in Fig. 1 (see the upper and lower traces, respectively). In Xe matrixes, the strongest bands for  $^{12}\text{C}_2\text{H}_2$  are at 3280.5, 3266.5, 1317, and  $727.5\text{ cm}^{-1}$  and in the case of  $^{13}\text{C}_2\text{H}_2$  the absorptions are at 3266.5, 1306.5, and  $726\text{ cm}^{-1}$ . These values agree with the spectrum of acetylene obtained by Maier and Lautz in solid Xe,<sup>20</sup> and when taking into account the normal matrix shift, with the acetylene spectra measured by Andrews, Johnson, and Kelsall in solid Ar.<sup>21</sup>

The 193 nm photolysis products of acetylene are presented in Table II. In solid Kr, the most prominent photolysis products of acetylene are  $\text{C}_2\text{H}$  radicals<sup>22</sup> and  $\text{KrHKr}^+$  ions.<sup>23</sup> The photodecomposition of acetylene at 193 nm in Xe matrixes produces  $\text{C}_2\text{H}$  radicals and  $\text{XeHXe}^+$  ions<sup>24</sup> similarly to the situation in a Kr matrix, and additionally the  $\text{C}_2$ -Xe compound is visible in the spectra.<sup>20</sup> The  $\text{C}_2\text{H}$  radicals are the primary photolysis product of acetylene, and photodissociation of  $\text{C}_2\text{H}$  produces  $\text{C}_2$  molecules.<sup>20</sup> Some formation of  $\text{C}_4$  clusters was also seen upon photolysis most probably from

TABLE II. 193 nm photolysis products (absorption wavenumbers in  $\text{cm}^{-1}$ ) of acetylene in Kr and Xe matrixes. The main photolysis products are in bold.

	Kr	Xe
$^{12}\text{C}^{12}\text{CH}$	1842	1852
$^{13}\text{C}^{13}\text{CH}$	1782	1791
$^{12}\text{C}^{12}\text{C-Xe}$	...	1767
$^{13}\text{C}^{13}\text{C-Xe}$	...	1699
$^{12}\text{C}_4$	1539.5	1536
$^{13}\text{C}_4$	1480	1477
$\text{KrHKr}^+$	852	...
	1008	
$\text{XeHXe}^+$	...	730.5
		842.5
		953

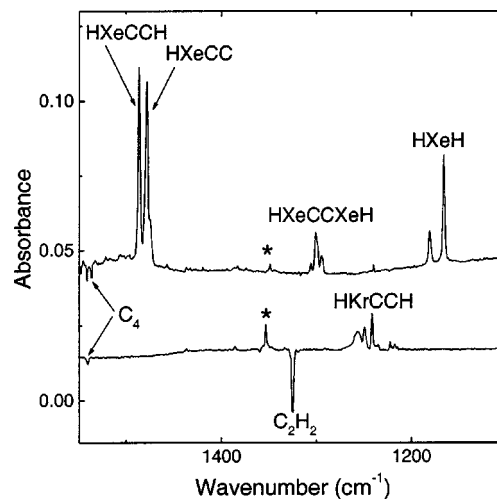


FIG. 2. Annealing-induced IR absorption spectra of Xe- and Kr-containing noble-gas compounds in the H-Ng stretching region. The acetylene/Ng samples ( $^{12}\text{C}$  compounds) were first irradiated at 193 nm and then annealed at 45 K for a Xe matrix (the upper trace) and at 30 K for a Kr matrix (the lower trace). The bands marked with an asterisk (\*) probably belong to the vinyl radical;  $\text{C}_2\text{H}_3$  (Ref. 29). The spectra are measured at 8 K.

acetylene dimers.<sup>25</sup> In some experiments with  $^{12}\text{C}_2\text{H}_2/\text{Xe}$  we used photolysis at 250 nm. The photolysis products are similar, but the  $\text{C}_2/\text{C}_2\text{H}$  ratio is larger upon irradiation at 250 nm than at 193 nm. The larger  $\text{C}_2/\text{C}_2\text{H}$  ratio leads in annealing to the more efficient formation of  $\text{HXeCC}$  radicals as compared with  $\text{HXeCCH}$ .<sup>6</sup> The photodecomposition of acetylene was more efficient in solid Xe (typically  $\sim 50\%$ – $80\%$ ) than in solid Kr ( $\sim 20\%$ – $30\%$ ) for similar light exposures at 193 nm (typically  $\sim 5000$  pulses with energy of  $20\text{ mJ/cm}^2$ ). This is probably connected with the fact that UV photolysis in noble-gas solid is often self-limited due to rising absorbers.<sup>26</sup> Annealing at 30 K of Kr matrixes and at 45 K of Xe matrixes efficiently mobilizes H atoms<sup>10</sup> and leads to the formation of various noble-gas molecules with characteristic H-Ng stretching bands ( $^{12}\text{C}$ ):  $\text{HKrCCH}$  [ $1256.6$ ,  $1249.6$ , and the strongest absorption (s) at  $1241.6\text{ cm}^{-1}$ ] in solid Kr and  $\text{HXeCCH}$  [ $1486.4$  (s) and  $1480.7\text{ cm}^{-1}$ ],  $\text{HXeCC}$  [ $1478.3$  (s) and  $1474.7\text{ cm}^{-1}$ ],  $\text{HXeCCXeH}$  [ $1305.8$ ,  $1300.9$  (s), and  $1294.3\text{ cm}^{-1}$ ], and  $\text{HXeH}$  [ $1166$  and  $1180\text{ cm}^{-1}$ ] in solid Xe.<sup>6,7</sup> The spectra of these molecules in the H-Ng stretching region are presented in Fig. 2 and the absorption wave numbers are given in Table III.

The  $^{13}\text{C}$  substitution shifts most of the absorptions of the organo-noble-gas molecules to lower energies (see Table III). For  $\text{HKrCCH}$ , the C-H stretching band shifts by  $-15.2\text{ cm}^{-1}$  (calculated value  $-16.8\text{ cm}^{-1}$ ). The C-C-H bending shift is  $-4.7$  and  $-5.0\text{ cm}^{-1}$  depending on the matrix site (calculated  $-5.9\text{ cm}^{-1}$ ). The H-Kr stretching shifts are from  $-1.0$  to  $-3.6\text{ cm}^{-1}$  (calculated  $-0.2\text{ cm}^{-1}$ ) as presented in Fig. 3. For  $\text{HXeCCH}$ , the observed shifts of the C-H stretching and C-C-H bending modes are similar to the Kr analog. By fitting the bands by Gaussian functions we obtained a small anomalous shift ( $+0.1$  and  $+0.2\text{ cm}^{-1}$ ) for the H-Xe stretches of  $\text{HXeCCH}$  (calculated  $-0.2\text{ cm}^{-1}$ ) upon  $^{13}\text{C}$  substitution. Similarly, the  $^{13}\text{C}$ -substitution-induced small anomalous shift was extracted for one of the H-Xe stretching

TABLE III. Experimental IR absorptions (in  $\text{cm}^{-1}$ ) of  $^{12}\text{C}/^{13}\text{C}$ -substituted  $\text{HNgCCH}$  ( $\text{Ng}=\text{Kr}$  or  $\text{Xe}$ ),  $\text{HXeCC}$ , and  $\text{HXeCCXeH}$ . The values for the  $^{12}\text{C}$  compounds correspond to the data in Refs. 6 and 7, but here the values are defined with better precision. The strongest absorptions are marked with (s).

	$\text{HKr}^{12}\text{C}^{12}\text{CH}$	$\text{HKr}^{13}\text{C}^{13}\text{CH}$	Shift ( $^{13}\text{C}$ )	$\text{HXe}^{12}\text{C}^{12}\text{CH}$	$\text{HXe}^{13}\text{C}^{13}\text{CH}$	Shift ( $^{13}\text{C}$ )
C-H stretch	3290.0	3274.8	-15.2	3273.0	3257.0	-16.0
H-Kr (Xe) stretch	1256.6	1255.6	-1.0	1486.4(s)	1486.5	+0.1
	1249.6	1246.5	-3.1	1480.7	1480.9	+0.2
	1241.6(s)	1238.0	-3.6			
C-C-H bend	610.2	605.2	-5.0	627.6	623.3	-4.3
	608.2	603.5	-4.7	625.7	621.5	-4.2
	$\text{HXe}^{12}\text{C}^{12}\text{C}$	$\text{HXe}^{13}\text{C}^{13}\text{C}$	Shift ( $^{13}\text{C}$ )	$\text{HXe}^{12}\text{C}^{12}\text{CXeH}$	$\text{HXe}^{13}\text{C}^{13}\text{CXeH}$	Shift ( $^{13}\text{C}$ )
H-Xe stretch	1478.3(s)	1478.1	-0.2	1305.8	a	...
	1474.7	1474.5	-0.2	1300.9(s)	1301.1	+0.2
				1294.3	1294.4	-0.1
C-C stretch	1748	1683	-65			

<sup>a</sup>Partially overlaps with a strong band of acetylene at  $1306.5\text{ cm}^{-1}$ .

bands of  $\text{HXeCCXeH}$  (see Fig. 4). The CC stretching mode of  $\text{HXeCC}$  shifts upon the  $^{13}\text{C}$  substitution by  $65\text{ cm}^{-1}$  down in energy (calculated  $-62.7\text{ cm}^{-1}$ ). For H-Xe stretches of  $\text{HXeCC}$  we extracted a small normal downshift of  $-0.2\text{ cm}^{-1}$ . We estimate that the experimental error in determination of the H-Xe stretching frequencies does not exceed  $0.1\text{ cm}^{-1}$ , however, the small shifts of  $0.1\text{--}0.2\text{ cm}^{-1}$  should be considered as tentative.

We have also measured formation kinetics of the noble-gas compounds upon annealing. The formation rate depends on the annealing temperature, as demonstrated in Fig. 5. The data are normalized by the values measured after additional annealing at 45 K, which stabilizes the processes connected with hydrogen mobility.<sup>10,12</sup> In this experiment, the 250 nm photolysis was used in order to enhance formation of  $\text{HXeCC}$  and  $\text{HXeCCXeH}$ . It is seen in Fig. 5 that the formation of  $\text{HXeCCXeH}$  is delayed as compared with  $\text{HXeH}$  and  $\text{HXeCC}$ . The difference in formation of  $\text{HXeCC}$  and

$\text{HXeCCXeH}$  can be explained by kinetic reasons rather than by the reaction barrier for  $\text{HXeCCXeH}$ . In this image, the formation of  $\text{HXeCCXeH}$  occurs in two steps involving  $\text{HXeCC}$  as an intermediate:



To confirm this mechanism, we irradiated the sample at 488 nm during annealing. The idea of this experiment is the following.  $\text{HXeCC}$  is very photolabile,<sup>6</sup> and it is efficiently bleached by 488 nm irradiation of an  $\text{Ar}^+$  laser (timescale  $\sim 1\text{ min}$  for laser intensity  $\sim 10\text{ mW/cm}^2$ ). The other annealing products ( $\text{HXeH}$ ,  $\text{HXeCCCH}$ , and  $\text{HXeCCXeH}$ ) are practically stable upon this irradiation. We found that this procedure (irradiation at 488 nm during annealing) totally destroys formation of  $\text{HXeCCXeH}$  (see Fig. 6), indicating that the formation of  $\text{HXeCCXeH}$  needs the  $\text{HXeCC}$  intermediate.

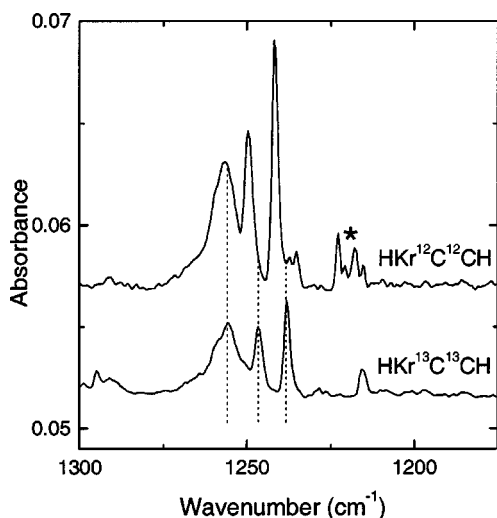


FIG. 3. Fragments of annealing-induced IR absorption spectra of  $\text{HKr}^{12}\text{C}^{12}\text{CH}$  and  $\text{HKr}^{13}\text{C}^{13}\text{CH}$  measured in a Kr matrix at 8 K. Note the effect of carbon isotopic substitution in the H-Kr stretching region. The vertical lines are for guiding the eye. The bands marked with an asterisk (\*) probably belong to other sites of  $\text{HKrCCH}$  or its complex. The participation of  $\text{HKrCCH}$  in these bands is suggested by selective photodecomposition.

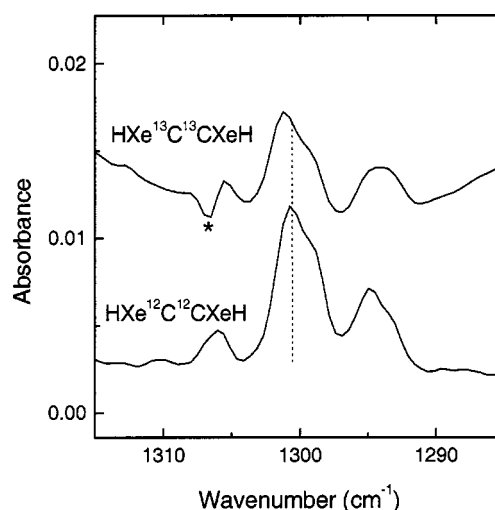


FIG. 4. The spectra of  $\text{HXe}^{12}\text{C}^{12}\text{CXeH}$  and  $\text{HXe}^{13}\text{C}^{13}\text{CXeH}$  in the H-Xe stretching region measured in a Xe matrix at 8 K. Note the small anomalous effect on the middle matrix site of the H-Xe stretching mode. The vertical line is for guiding the eye. The negative feature marked with an asterisk (\*) is from  $^{13}\text{C}_2\text{H}_2$ .

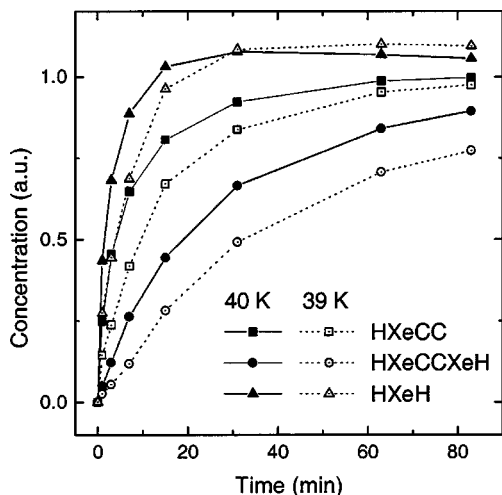


FIG. 5. Formation kinetics of HXeCC, HXeCCXeH, and HXeH at 39 and 40 K in solid Xe. Before annealing the acetylene/Xe samples were photolyzed at 250 nm which produced CC molecules in large amounts and CCH radicals in minor amounts. The relative concentrations of HXeCC, HXeCCXeH, and HXeH are obtained by integrating the 1478.3, 1300.9 and 1180, 1166  $\text{cm}^{-1}$  absorption bands and normalized by the values obtained after additional annealing at 45 K, which stabilizes the processes connected with hydrogen mobility. In this experiment, HXeCCH is formed in relatively small amounts. The spectra are measured at 8 K.

#### IV. DISCUSSION

##### A. $^{13}\text{C}$ isotope effect

Our motivation for  $^{13}\text{C}$  substitution experiments was twofold. First, we wanted to confirm the assignment of the organo-noble-gas molecules done previously.<sup>6,7</sup> Second, it was interesting to study heavy-atom isotope shift of the H-Ng stretching modes because the  $^{18}\text{O}$  substitution led to anomalous shifts for HXeOH and HXeO and the effect was

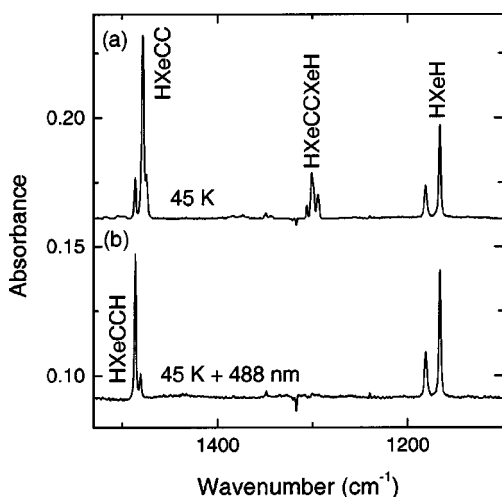


FIG. 6. IR absorption spectra of Xe-containing compounds prepared from  $^{12}\text{C}_2\text{H}_2/\text{Xe}$ . The samples were photolyzed at 250 nm and then annealed during  $\sim 60$  min at 40 K and then during  $\sim 3$  min at 45 K [the upper spectrum (a)]. The lower spectrum (b) was prepared in a similar way, but the sample was irradiated at 488 nm during annealing. The 488 nm radiation efficiently destroys HXeCC, but it does not essentially decompose HXeCCH and HXeCCXeH. The spectra were measured at 8 K. The absorptions of HXeCC and HXeCCH are doublets with wave numbers of 1478.3 and 1474.7  $\text{cm}^{-1}$  for HXeCC and 1486.4 and 1480.9  $\text{cm}^{-1}$  for HXeCCH.

described in terms of anharmonic coupling between the normal modes.<sup>5,15</sup> The experiments with  $^{13}\text{C}$ -substituted samples confirm the previous assignments taking into account the present computational data. As it can be seen in Tables I and III, the C-H stretching mode shifts experimentally 15.2 and 16.0  $\text{cm}^{-1}$  down in energy for HKrCCH and HXeCCH, respectively, in agreement with the calculated value of  $-16.8$   $\text{cm}^{-1}$ . The shifts of the C-C-H bending modes of HKrCCH and HXeCCH ( $-5.0$  and  $-4.7$   $\text{cm}^{-1}$  for Kr and  $-4.3$  and  $-4.2$   $\text{cm}^{-1}$  for Xe) also correspond to the calculated values ( $-5.9$  and  $-5.7$   $\text{cm}^{-1}$ , respectively). The C-C stretching mode of HXeCC shifts experimentally down in energy by 65  $\text{cm}^{-1}$ , which is in a good agreement with the calculated value ( $-62.7$   $\text{cm}^{-1}$ ). As a conclusion, the experimental results of the vibrational modes not directly involving noble-gas atoms (like C-H stretching, C-C stretching, and C-C-H bending) are in very good agreement with the harmonic estimates.

The correspondence of the calculations and the experimental results for the H-Kr and H-Xe stretches of these organo-noble-gas molecules is not so straightforward as for the modes discussed above. For the H-Kr stretching mode of HKrCCH, the harmonic calculations give  $-0.21$   $\text{cm}^{-1}$  for the shift upon  $^{13}\text{C}$  isotope substitution whereas experimentally the shift is measured to be from  $-1.0$  to  $-3.6$   $\text{cm}^{-1}$  depending on the matrix site (see Fig. 3). A similar numerical discrepancy between harmonic calculations and experimental results was observed previously in the  $^{18}\text{O}$  isotope substitution experiments on DXeOD.<sup>15</sup> For both HKrCCH and DXeOD, the harmonic approximation predicted small downshifts ( $-0.03$  to  $-0.2$   $\text{cm}^{-1}$ ) upon substitution with the heavier isotope ( $^{18}\text{O}$  or  $^{13}\text{C}$ ), which disagreed quantitatively with the experiments giving quite larger values (up to  $\sim -3$   $\text{cm}^{-1}$ ).<sup>15</sup> In the case of DXeOD, the calculations were previously performed using the anharmonic CC-VSCF theory.<sup>15</sup> Those calculations predicted for DXeOD relatively large downshift of 1.28  $\text{cm}^{-1}$ , which was closer to the experimentally observed downshift of 3.03  $\text{cm}^{-1}$ .<sup>15</sup> The observed quite large shifts of the H-Kr stretching mode of HKrCCH is probably due to anharmonic mode coupling similarly to the case of DXeOD.<sup>15</sup>

The H-Xe stretches of HXeCCH and one of the H-Xe stretch matrix sites of HXeCCXeH show small blueshifts upon the  $^{13}\text{C}$  isotope substitution. For HXeCC, we observed a downshift of  $-0.2$   $\text{cm}^{-1}$  for the H-Xe stretching mode. The harmonic calculations predict the  $^{13}\text{C}$  substitution-induced shifts of  $-0.4$ ,  $-0.1$ , and  $-0.2$   $\text{cm}^{-1}$  for HXeCC, HXeCCH, and HXeCCXeH, respectively (Table I). As we learned previously from the case of HXeOH, anomalous isotope shifts cannot be understood in the framework of the harmonic vibrational theory, since the anharmonic coupling between normal modes is needed to obtain both qualitative and quantitative agreement with the experimental findings.<sup>15</sup> We did not perform anharmonic calculations for the molecules studied here because of their computational complexity. It should be remembered that the possible anomalous effect due to anharmonic mode coupling always competes with the reduced-mass effect, and the anomalous result can occur only when the latter effect is small, and the Xe-containing compound is

a representative case. We claim the  $^{13}\text{C}$  isotope effect for the Xe compounds only tentatively. The reason for the uncertainty is a comparable experimental error ( $\sim 0.1 \text{ cm}^{-1}$ ). The absorption bands of the H-Xe stretching mode of HXeCCH and HXeCC overlap with each other, and the absorptions of both molecules are doublets which complicates the fitting procedure. By using the method of selective photolysis, we have been able to separate absorptions of HXeCCH and HXeCC (see Fig. 6). In the case of HXeCCXeH, the H-Xe stretching absorption bands are of a complicated shape (see Fig. 4) and an absorption band of  $\text{H}^{13}\text{C}^{13}\text{CH}$  is in the same region. In addition, the relative difference in masses is larger for  $^{16}\text{O}/^{18}\text{O}$  substitution than in the case of  $^{12}\text{C}$  and  $^{13}\text{C}$ , which makes the isotope effect for the oxygen compounds more pronounced.

## B. Evidence of the HXeCC+Xe+H reaction

Now we discuss the formation mechanism of the HXeCCXeH molecule in a Xe matrix. The formation may occur via two possible reactions:



The first reaction involves HXeCC as a precursor (model A), and the second reaction occurs via “a triple collision” of two mobile H atoms with an immobile CC molecule in Xe lattice (model B). It should be reminded that Xe atoms are always available for the reaction because the process is considered in Xe surrounding.

We model these two situations based on kinetic equations describing diffusion of H atoms in the lattice and the  $\text{H} + \text{Ng} + \text{Y}$  formation reactions as we successfully did previously for other HNgY molecules.<sup>13,14</sup> In this model, the formation kinetics of the HNgY molecule is described as

$$\frac{d[\text{HNgY}]}{dt} = k_1[\text{H}][\text{Y}] - k_2[\text{H}][\text{HNgY}], \quad (5)$$

where  $k_1$  and  $k_2$  are the rate constants. For simplicity, we assume here that the HCC radicals are absent in the matrix after photolysis meaning that HXeCCH molecules do not form upon annealing. This assumption is reasonable for the case of photolysis at 250 nm when the formation of CC molecules dominate over CCH radicals.<sup>6</sup> As the next simplification, we neglect here decomposition reactions of the formed HXeCC radicals and the HXeCCXeH molecules with mobile H atoms [the second term in Eq. (5)]. Indeed, these reactions most probably take place and particularly lead to formation of  $\text{H}_2$  molecules, however, they do not change qualitatively the formation kinetics.<sup>13,14</sup> The formation of HXeH, HXeCC, and HXeCCXeH is considered to possess the same reaction cross section, which is also an approximation. The HCC radicals are not recovered because the HXeCC channel protects their formation, in agreement with the experimental observations.

The result of the modeling is presented in Fig. 7. Plot (a) corresponds to model A relying on reaction (3) and the initial conditions  $[\text{H}]_0 = 2$ ,  $[\text{CC}]_0 = 1$ , the other initial concentrations being zero. Upon activation of hydrogen mobility, we

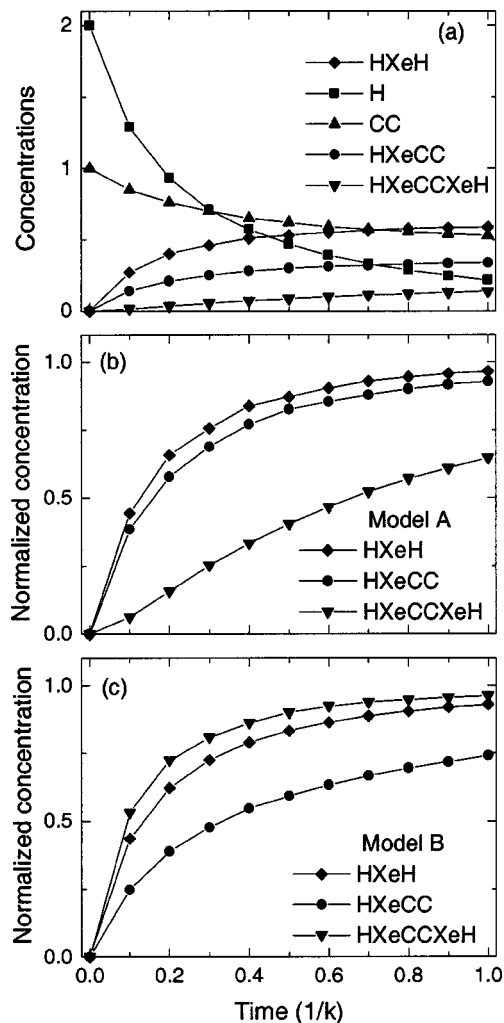


FIG. 7. Modeling of the HXeCCXeH formation mechanism. In plot (a) shown are the concentrations of HXeCC, HXeCCXeH, and HXeH as a function of annealing time using model A that relays on reaction (3). The initial conditions:  $[\text{H}]_0 = 2$ ,  $[\text{CC}]_0 = 1$ , and the other initial concentrations being zero. Plot (b) presents the results of the same calculations as in plot (a) modified in the way that the concentrations are normalized by their values after long annealing. Plot (c) describes the formation process based on model B relying on reaction (4), and the normalized concentrations of the annealing products are shown.

see formation of noble-gas molecules and a decrease of the H and CC concentrations. About 60% of CC molecules are consumed in the HXeCC and HXeCCXeH products when all H atoms have reacted, which corresponds to the experimental case of long annealing. Figure 7(b) presents the results of the same calculations modified in the way that the noble-gas products are normalized by their concentrations after long annealing. This normalization is useful in order to compare the shapes of the calculated kinetic curves and to compare them with the experimental dependencies when the actual concentrations are unknown. It is seen in plot (b) that HXeH possess the fastest formation whereas HXeCCXeH shows the slowest formation. The latter fact is connected with the assumed formation of HXeCCXeH from HXeCC [reaction (3)]. Indeed, HXeCC molecules are absent in the early stage of annealing, and the HXeCCXeH formation rate that is proportional to the HXeCC concentration is very small.

Figure 7(c) presents the formation kinetics based on model *B*, the normalized concentrations of the products being shown. As a strong qualitative difference from model *A*, model *B* gives very fast formation of HXeCCXeH from the beginning, and this originates from the requirement of triple collisions that are the most efficient at the early annealing stage when the H and CC concentrations are the highest. In fact, the HXeCCXeH concentration curve saturates here faster than the dependence for HXeH, which is due to the additional contribution of the decreasing CC concentration. The relative amount of the HXeCCXeH product predicted by the model depends on the probability of triple H+CC+H collisions [reaction (4)] in a suitable geometry configuration, and its value is difficult to be estimated. In the present calculation we actually assumed this probability to be five times smaller than that of double H+CC collisions (for the unit concentration). The qualitative kinetic behavior is quite insensitive to this probability factor.

The comparison of the modeling results with the experimental data (see Fig. 5) strongly favors model *A*. As a fingerprint, the experimental HXeCCXeH formation is the slowest among the products. In order to make numerical comparison, we can consider the annealing periods needed to reach 50% of the final product concentration. The ratio of these periods for HXeCCXeH and HXeH products is 5.5 based on model *A* and it is from 8.1 to 12.4 in the experiments, which should be considered as a good agreement. Model *B* yields the controversial value of 0.7. The validity of model *A* is further supported by our experiments with annealing upon irradiation at 488 nm. This radiation selectively destroys HXeCC. Based on model *A*, the irradiation at 488 nm should prevent formation of the HXeCCXeH molecules because of the absence of the HXeCC intermediate, and this is exactly what we observed experimentally (see Fig. 6). In contrast, model *B* gives an increase of the HXeCCXeH concentration upon selective decomposition of HXeCC. These facts mean that the HXeCCXeH formation needs HXeCC as a precursor, i.e., the HXeCCXeH molecules are formed in our experiments via reaction (3).

Reaction (3) offers the first example of an additive chemical reaction involving HNgY molecules, which is qualitatively different from the decomposition reactions (H+HXeH and H+HKrCl) reported previously.<sup>13,14</sup> In this case, a reaction of one noble-gas molecule (HXeCC) produces another noble-gas molecule (HXeCCXeH). This makes a remarkable case of low-temperature chemical synthesis of noble-gas compounds. We have demonstrated that it is possible to react a HNgY molecule and form another metastable noble-gas species. This result seems to be not obvious because of a very large energy accumulated in the

HXeCCXeH molecule with respect to acetylene (computationally  $\sim 9.3$  eV!).<sup>19</sup> The observed formation of HXeCCXeH shows in particular that the bending barriers are high enough to prevent the path to the lower energy minima with formation of HXeCCH or HCCH. It should be noticed in this respect that the HXeCCXeH molecules appear in our experiments in good amounts despite their formation from HXeCC. If we rely on the computational IR intensities of the H-Xe

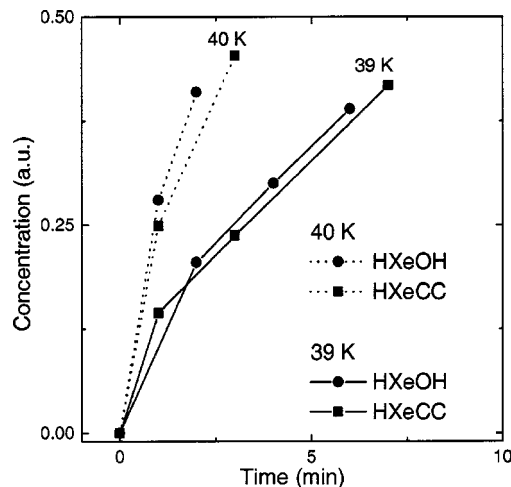


FIG. 8. Comparison of the HXeCC and HXeOH formation in the early annealing stage (data for HXeOH is from Ref. 12) in solid Xe. Data for two annealing temperatures (39 and 40 K) are presented. Before annealing the samples were photolyzed at 193 nm ( $\text{H}_2\text{O}/\text{Xe}$ ) and 250 nm ( $\text{C}_2\text{H}_2/\text{Xe}$ ). The concentrations are obtained from integration of the 1478.3 (HXeCC) and 1578 (HXeOH)  $\text{cm}^{-1}$  bands and normalized by the values obtained after additional annealing at 45 K. The spectra are measured at 8 K.

stretching modes (2503 and 5451  $\text{km}/\text{mol}$  for HXeH (Ref. 27) and HXeCCXeH,<sup>19</sup> respectively), we find that the HXeCCXeH concentration is 36–42% of the HXeH concentration, which reasonably agree with the estimates of model *A* (23%). The observed agreement between the experiment and the simple kinetic model particularly shows that the cross section of various reactions involved in the kinetic scheme do not differ much from each other, i.e., they are quite comparable.

The formation of HNgY molecules is a diffusion-controlled process as has been demonstrated previously for example, for HXeOH and HKrCl.<sup>12,13</sup> We have studied the formation kinetics of HXeCC and found that it is similar to HXeOH as it can be seen in Fig. 8. HXeCC and HXeOH start increasing in annealing very synchronously and with similar efficiency (see Fig. 8). This means that the activation energy is practically the same for the HXeCC and HXeOH formation so that the chemical reaction barriers are negligible at annealing temperatures  $\sim 40$  K. This conclusion is presumably applicable for other HNgY molecules as well. The experiments have shown that various HXeY molecules are formed at the same annealing temperature ( $\sim 40$  K), which would not be the case if the reaction activation energy were important.<sup>3,12</sup> In addition, the formation of HXeCl and HXeBr in solid Ne at 12 K supports the very low intrinsic formation barriers of the HNgY molecules.<sup>28</sup>

## V. CONCLUSIONS

The measured kinetics of the organo-noble-gas compounds features their diffusion-controlled formation. The formation of HXeCCXeH is delayed compared with other Xe-containing species (HXeH, HXeCC, and HXeCCH). The experimental data can be explained using a model assuming that formation of HXeCCXeH needs HXeCC as a reaction precursor. This makes an example of a constructive reaction

involving HNgY molecules where a reaction of one noble-gas molecule (HXeCC) produces another noble-gas molecule (HXeCCXeH).

Experiments with  $^{13}\text{C}$ -substituted samples confirmed the previous assignments of these molecules (HKrCCH, HXeCC, HXeCCH, and HXeCCXeH). The harmonic vibrational calculations performed here agree with the experimental results with respect to the C-H stretching, C-C-H bending, and C-C stretching modes. The tentative anomalous isotope effect on H-Xe stretching modes of HXeCCH and HXeCCXeH was found experimentally. The situation with these molecules is similar to the previously studied  $^{18}\text{O}$  substitution in HXeOH, HXeOD, and HXeO.<sup>5,15</sup> For HKrCCH, we observed a pronounced effect of the  $^{13}\text{C}$  substitution on the H-Kr stretching mode (downshift by 1.0–3.6  $\text{cm}^{-1}$ ), which is similar to the case of DXeOD.<sup>15</sup> The observed shifts for the H-Ng stretching frequency are presumably connected with the anharmonic mode coupling.

#### ACKNOWLEDGMENT

The Academy of Finland supported this work. H. T. thanks Magnus Ehrnrooth's foundation for financial support.

- <sup>1</sup>M. Pettersson, J. Lundell, and M. Räsänen, *J. Chem. Phys.* **102**, 6423 (1995).
- <sup>2</sup>M. Pettersson, J. Lundell, and M. Räsänen, *Eur. J. Inorg. Chem.* 729 (1999).
- <sup>3</sup>J. Lundell, L. Khriachtchev, M. Pettersson, and M. Räsänen, *J. Low Temp. Phys.* **26**, 680 (2000).
- <sup>4</sup>L. Khriachtchev, M. Pettersson, N. Runeberg, J. Lundell, and M. Räsänen, *Nature (London)* **406**, 874 (2000).
- <sup>5</sup>L. Khriachtchev, M. Pettersson, J. Lundell, H. Tanskanen, T. Kiviniemi, N. Runeberg, and M. Räsänen, *J. Am. Chem. Soc.* **125**, 1454 (2003).
- <sup>6</sup>L. Khriachtchev, H. Tanskanen, J. Lundell, M. Pettersson, H. Kiljunen, and M. Räsänen, *J. Am. Chem. Soc.* **125**, 4696 (2003).
- <sup>7</sup>L. Khriachtchev, H. Tanskanen, A. Cohen, R. B. Gerber, J. Lundell, M. Pettersson, H. Kiljunen, and M. Räsänen, *J. Am. Chem. Soc.* **125**, 6876 (2003).
- <sup>8</sup>H. Tanskanen, L. Khriachtchev, J. Lundell, H. Kiljunen, and M. Räsänen, *J. Am. Chem. Soc.* **125**, 16361 (2003).
- <sup>9</sup>V. I. Feldman, F. F. Sukhov, A. Y. Orlov, and I. V. Tyulpina, *J. Am. Chem. Soc.* **125**, 4698 (2003).
- <sup>10</sup>J. Eberlein and M. Creutzburg, *J. Chem. Phys.* **106**, 2188 (1997).
- <sup>11</sup>K. Vaskonen, J. Eloranta, T. Kiljunen, and H. Kunttu, *J. Chem. Phys.* **110**, 2122 (1999).
- <sup>12</sup>L. Khriachtchev, H. Tanskanen, M. Pettersson, M. Räsänen, V. Feldman, F. Sukhov, A. Orlov, and A. F. Shestakov, *J. Chem. Phys.* **116**, 5708 (2002).
- <sup>13</sup>L. Khriachtchev, M. Saarelainen, M. Pettersson, and M. Räsänen, *J. Chem. Phys.* **118**, 6403 (2003).
- <sup>14</sup>L. Khriachtchev, M. Pettersson, H. Tanskanen, and M. Räsänen, *Chem. Phys. Lett.* **359**, 135 (2002).
- <sup>15</sup>L. Khriachtchev, J. Lundell, M. Pettersson, H. Tanskanen, and M. Räsänen, *J. Chem. Phys.* **116**, 4758 (2002).
- <sup>16</sup>H.-G. Yu and J. T. Muckerman, *J. Theor. Comp. Chem.* **2**, 573 (2003).
- <sup>17</sup>M. J. Frisch, G. W. Trucks, H. B. Schlegel *et al.*, GAUSSIAN98, Revision A.11.4, Gaussian, Inc., Pittsburgh PA, 2002.
- <sup>18</sup>L. A. LaJohn, P. A. Christiansen, R. B. Ross, T. Atashroo, and W. C. Elmer, *J. Chem. Phys.* **87**, 2812 (1987).
- <sup>19</sup>J. Lundell, A. Cohen, and R. B. Gerber, *J. Phys. Chem. A* **106**, 11950 (2002).
- <sup>20</sup>G. Maier and C. Lautz, *Eur. J. Inorg. Chem.* 769 (1998).
- <sup>21</sup>L. Andrews, G. L. Johnson, and B. J. Kelsall, *J. Phys. Chem.* **86**, 3374 (1982).
- <sup>22</sup>D. Forney, M. E. Jacox, and W. E. Thomson, *J. Mol. Spectrosc.* **170**, 178 (1995).
- <sup>23</sup>V. E. Bondybey and G. C. Pimentel, *J. Chem. Phys.* **56**, 3832 (1972).
- <sup>24</sup>H. Kunttu, J. Seetula, M. Räsänen, and V. A. Apkarian, *J. Chem. Phys.* **96**, 5630 (1992).
- <sup>25</sup>J. Szczepanski, S. Ekern, C. Chapo, and M. Vala, *Chem. Phys.* **211**, 359 (1996).
- <sup>26</sup>L. Khriachtchev, M. Pettersson, and M. Räsänen, *Chem. Phys. Lett.* **288**, 727 (1998).
- <sup>27</sup>J. Lundell, G. M. Chaban, and R. B. Gerber, *J. Phys. Chem. A* **104**, 7944 (2000).
- <sup>28</sup>M. Lorenz, M. Räsänen, and V. E. Bondybey, *J. Phys. Chem. A* **104**, 3770 (2000).
- <sup>29</sup>R. A. Shepherd, T. J. Doyle, and W. R. M. Graham, *J. Chem. Phys.* **89**, 2738 (1988).